Int. J. Nonlinear Anal. Appl. 13 (2022) 2, 3127–3137
ISSN: 2008-6822 (electronic)
http://dx.doi.org/10.22075/ijnaa.2022.6783

Electric quadrupole transition in neutron rich $^{32-42}$S-isotopes with different model spaces

A. A. Abdulhasan*, Z. A. Dakhil*

Department of Physics, College of Science, University of Baghdad, Iraq

(Communicated by Javad Vahidi)

Abstract

The electromagnetic properties of some even neutron rich Sulfur-isotopes $^{32-42}$ S are studied through the electric quadrupole transition $(0_1^+ \to 2_1^+)$. In particular, excitation energies E_x, occupancies, electric quadrupole moments Q, transition strengths $B(E2)$, deformation parameters β_2 and the coulomb inelastic electron scattering form factors are calculated for the adopted isotopes within the framework of shell model. The shell model calculations are performed with full *sd*-model space, *psd* - and *sdpf* - cross shell, using different interactions. The results are based on *sdba* and *psdmk* interactions for sulfur with $N \leq 20$, while sdpfk and *sdpfu* interactions are dependent for sulfur with $N > 20$. The core polarization effects (CP) are included through the Boher-Mottelson $(B - M)$ and standard (ST) effective charges to obtain a reasonable description of the electric quadrupole moments and C2 form factors. The results of *psdmk* and *sdba*-interactions fail to reproduce the measured $B(E2)$ strengths and deformation β_2 for $^{32-36}$ S, except for ^{36} S nucleus is close to the measured value. The results for $^{38-42}$ S with both *sdpfk* and *sdpfu* interactions nicely confirm the measured values of $B(E2)$ strengths and deformation β_2 within the experimental error. The influence of the nuclear deformation parameter β_2 on the location of the diffraction minima of C2 form factors are also indicated.

Keywords: Excited energy, Quadrupole moments, effective charges, Deformation parameters, Reduced transition probabilities, Electron scattering form factor
2020 MSC: 78A15

1 Introduction

Exotic feature in nuclear physics is of tremendous interest not only because it serves as a rigorous test for existing nuclear models, but also because it opens up new study fields in nuclear science. Also, because it cannot only discover new nuclear properties and thereby enrich our knowledge of atomic nuclei, but also allows understanding the nucleon-synthesis origin of chemical elements [32]. The interest for exotic nuclei has increased enormously since the recent progress in nuclear accelerators. The electron scattering from neutron rich nuclei has received wide attention from researchers especially in the theoretical studies due to the importance of this process as a probe for the study of nuclear structure. The electromagnetic moments are one of the main probes to gain information about the nuclear structure throughout the entire nuclear chart. The quadrupole moment is a unique instrument to study the deformation and collective behavior of nuclei both at low and high excitation energy [8, 13]. In the present work, we mainly concerned on the structure of $(0_1^+ \to 2_1^+)$ transition in neutron-rich of even-even sulfur isotopes. The neutron-rich sulfur isotopes

*Corresponding author
Email addresses: ali.hamza1104@sc.uobaghdad.edu.iq (A. A. Abdulhasan), zahida.a@sc.uobaghdad.edu.iq (Z. A. Dakhil)

Received: November 2021 *Accepted:* March 2022

have a remarkable amount of theoretical and experimental attention, which has provided significant information on the evolution of nuclear properties with shell model studies and into the modification of the nuclear shell structure far from the stability line. The reduced transition probabilities *B(E2)* are necessary for nuclear structural information, corresponding to information about the energies of low-lying levels in even-even nuclei. They have emphasized the extensive occurrence of quadrupole deformation in nuclei [26]. Many theoretical calculations have explored the role of effective charges on quadrupole moments and B(E2) strengths [12, 29, 20, 17]. The energies and B(E2) strengths from the ground state of 2^+ levels beyond the lowest energy 2^+ states for ^{38,40,42}S[25] and ^{44} S[10] were first measured using the intermediate energy coulomb excitation over 20 years ago. They compared their data to the results of Werner et al. [30], which using self-consistent mean field techniques and also compared to the shell model using empirical interactions. Recently, Longfellow et al. [14] reported the second measurements of the $B(E2:0^+\rightarrow 2^+)$ strength using the experimental techniques described in [25, 10] with the increase in secondary beams rates available to populate both the first and higher-lying 2^+ levels in S-isotopes from $N=22-28$. They compared their data to the predictions from shell model calculations using SDPF-MU interaction. In general, their results of B(*E2*) strengths are slightly lower than those of previous work published by Scheit et al. [25] and Glasmacher et al. [10]. In the present work, we will report the predicted values of energies, occupancies, B($E2:0^+\rightarrow 2^+$) strengths, the quadrupole moments and the deformation parameters, furthermore, the C2 form factors for even-even neutron-rich sulfur isotopes $^{32-42}$S within the framework of shell model. The shell model calculations using different model spaces, psd, sd and sdpf-model spaces are adopted. The single particle wave functions of harmonic oscillator with size parameter b are used. The core polarization effects are included through different effective charges (e_{eff}). The standard (ST) effective charges of Ref. [22] and Bohr-Mottelson ($B-M$) effective charges [1] are dependent.

2 Theoretical Formalism

The many-particles reduced matrix elements of longitudinal electron scattering operator T^{coul}_{LT} operator between the initial (i) and the final (f) states for a given multipolarity L can be expressed as the sum of the products of the one-body density matrix (OBDM) times the reduced single-particle matrix elements [8, 6]:

$$\left\langle J_f T_f \left\| \hat{T}^{\text{coul}}_{L,T}\left(q\right)\right\| J_i T_i\right\rangle = \sum_{a,b} OBDM\left(L,J_f,J_i,a,b,t_z\right)\left\langle a\left\|\hat{T}^{\text{coul}}_{L,t_z}\left(q\right)\right\| b\right\rangle \tag{2.1}$$

The reduced single-particle matrix elements $\langle||\ ||\rangle$ between the final $|a\rangle$ state and the initial state $|b\rangle$ is given by [6]:

$$\left\langle a\left\|\widehat{T}^{\text{coul}}_{L,t_z}\right\| b\right\rangle = e\left(t_z\right)\left\langle n_a\ell_a\left|j_L(qr)\right|n_b\ell_b\right\rangle\left\langle \ell_a\frac{1}{2}j_a\left\|Y_L\left(\Omega_r\right)\right\|\ell_b\frac{1}{2}j_b\right\rangle \tag{2.2}$$

Where $j_L(qr)$ is the spherical Bessel function $Y_{LM}(\Omega_r)$, is the spherical harmonics function, and $e(t_z)=\frac{1+\tau_z(i)}{2}, \tau_z = 2t_z$, the reduced single-particle matrix elements $\langle||\ ||\rangle$ used in the present work are those of Brown et al. [31].The longitudinal electron scattering form factor for multipolarity L and momentum transfer q, between the initial and final nuclear states of spin $J_{i,f}$ and isospin $T_{i,f}$ is given by [7, 6]:

$$\left|F^{\text{coul}}_L\left(q\right)\right|^2 = \frac{4\pi}{\left(2J_i+1\right)Z^2}\left|\sum_{T=0,1}(1-)^{T_f-T_{zf}}\begin{pmatrix} T_f & T & T_i\\ -T_{zf} & 0 & T_{zi}\end{pmatrix}\left\langle J_fT_f\left\|\boldsymbol{P}^{\text{coul}}_L\left(q\right)\right\| J_iT_i\right\rangle F_{c.m.}(q)F_{f.s.}(q)\right|^2 \tag{2.3}$$

The normalization, $(4\pi/Z^2)$, ensures that the longitudinal elastic scattering form factor equates to unity at photon point. Since the Hamiltonian in shell model is in general not translation invariant, the center of mass correction is $F_{c.m.}=e^{\frac{q^2b^2}{4A}}$ [28, 9], where (b) is the harmonic oscillator length parameter, and (A) is the mass number. The finite size (f.s.) form factor is [11], $F_{f.s.}(q)=[1+(q/4.33)^2]^{-2}$. The Coulomb distortion of the electrons increases the momentum transfer q. These effects can be included by replacing the momentum transfer q with an effective one $\vec{q}_{eff}$ [7]: $q_{eff}=q[1+\frac{3Ze^2}{2E_iR_c}]$, Where, E is the electron energy and $R_c=\sqrt{\frac{5}{3}}r_{rms}\approx 1.2A^{1/3}fm$, and $e^2=\alpha\hbar c=1.44MeV.fm, (r_{rms})$ is the root mean square charge radii. The multipolarity (L) is determined from the parity and angular momentum selection rules: $\Delta\pi^{El}=(-1)^L, \Delta\pi^m=(-1)^{L+1}, |J_i-J_f|\leq L\leq J_i+J_f$.

The electric quadrupole moment in a state $|L=2,M=0\rangle$ for $J_i=J_f$ is defined as [5]:

$$Q = \begin{pmatrix} J_i & 2 & J_i \\ -J_i & 0 & J_i \end{pmatrix} \sqrt{\frac{16\pi}{5}} \left\langle J_i \| \hat{O}(E2) \| J_i \right\rangle \tag{2.4}$$

Where, $\langle J_i \hat{O}(E2) J_i \rangle$ is the nuclear matrix element of the electromagnetic operators.

The form factor is related to the reduced transition probability at the photon point as [31],

$$B(EL) = \frac{[(2L+1)!!]^2 Z^2 e^2}{4\pi k^{2L}} |F_L(q=k)|^2 \tag{2.5}$$

Where $k = E_x/\hbar c, B(E2)$ in unit of $e^2 fm^4$, and Q in unit of efm^2.

The quadrupole moment is related to the reduced transition probability B(EL) by [31],

$$Q = \begin{pmatrix} J_i & 2 & J_i \\ -J_i & 0 & J_i \end{pmatrix} \sqrt{\frac{16\pi}{5}} \sqrt{(2J_i+1)\, B(E2)} \tag{2.6}$$

The deformation parameter (β_2) is used to describe the shape of the axially symmetric deformed nucleus. The quadruple deformation parameter (β_2) is also related to reduced transition probability B($E2$) by [10]:

$$\beta_2 = \frac{4\pi}{3ZR_c^2} \left[\frac{B(E2)}{e^2}\right]^{\frac{1}{2}} \tag{2.7}$$

3 Result and discussion

A detailed study has been done for even-even sulfur isotopes. The present work is focused on the electric quadrupole transition from the ground state to first 2_1^+ excited state ($0_1^+ \to 2_1^+$). The calculations are performed with different model spaces using the shell model code OXBASH [4] to obtain the *(OBDM)* elements and energy levels. The results are based on *sdba* and *psdmk* interactions [15], for sulfur with $N \leq 20$, while *sdpfk* and *sdpfu* interactions [12, 16] are dependent for sulfur with $N < 20$.The single particle wave functions of HO potential are used with the size parameter (b) obtained from the global formula for oscillator length [2]:

$$b = \sqrt{\frac{\hbar}{M_p w}} \text{ with } \hbar w = 45A^{-1/3} - 25A^{-2/3}$$

The shell model calculations of $^{32-42}$S isotopes are included the excited energies, the quadrupole moments *(Q)*, transition strengths B(*E2*), deformation parameters (β_2) and occupancies of $0_1^+ \to 2_1^+$ transition. Furthermore, the C2 form factors are also calculated. In general, one can notice here as well as for all other (Q) observables in the *sd*-shell nuclei that the measured moments are systematically larger than those calculated with bare nucleon charges. This is due to the well-known effect of the polarization of the core protons by the valance protons and neutrons [3, 23]. This effect is calculated by replacing the free nucleon charges with the effective charges $\delta e(t_z)$. Bohr-Mottelson *(B-M)* [1] formulated an expression for effective charges to explicitly include neutron excess via,

$e^{eff}(t_z) = e(t_z) + \delta e(t_z)$

$\delta e(t_z) = Z/A - 0.32(N-Z)/A - 2t_z[0.32 - 0.3(N-Z)/A]$

The sensitivity of Q moments to the values of the effective charges is also presented with $\left(e_p^{eff} = 1.36e,\ e_n^{\text{eff}} = 0.45e\right)$ as standard effective charge ST [22].

The calculated excitation energies E_x for $^{32-36}$ S-isotopes with *sdba* and *psdmk* interactions are listed in table (1) together with the measured values [28] for comparison. The excitation energies $E_x = \left(2_1^+\right)$are calculated with *psdfk*-interaction for *psd* cross-shell and with *sdba*-interaction for *sd*-shell.

In Fig. (1), the predicted E_x with different interactions are compared with experimental data [28] (black circles). For ^{34} S with the result with the *psdmk* interaction ($E_x = 2.292$MeV) gives good agreement with the experimental data ($E_{\text{exp}} = 2.127 \pm 13$MeV), and is better than those for both ^{32} S ($E_x = 3.613$MeV) and ^{36} S ($E_x = 6.275$MeV). These results for ^{32,36} S are by far the largest in this mass region. The value of ^{36} S is about a factor of two larger than the measured value. This difference is related to high energy gap for ^{36} S nucleus which has neutron magic

number ($N = 20$). In the region of A $\geq$ 38 (with N > 20) the results with both $sdpfk$ and $sdpfu$ interactions are well reproduced the correct 2_1^+ excited energy.

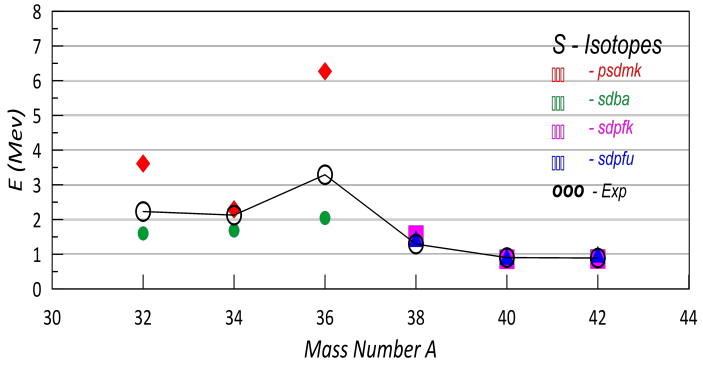

Figure 1: Excitation energies of even-even S-isotopes in the excited state 2_1^+ states. The experimental data are taken from Ref [18].

For ^{32,34,36} S, the occupancies of $1d_{5/2}, 2s_{1/2}$ and $1d_{3/2}$ the valence proton and neutron orbital with $sdba-$ interaction are shown in Fig.(2-a) with configuration $(1s)^4(1p)^{12}$ inert core. For configuration $(1s)^4$ inert core, the occupancies of $1p_{3/2}, 1p_{1/2}, 1d_{5/2}, 2s_{1/2}$ and $1d_{3/2}$ proton and neutron orbital with psdmkinteraction are shown in Fig.(2-b). In general, the role of $1d_{5/2}$ orbital is important as the neutrons number is increased as well as other sd-shell nuclei [24]. The contribution of neutron occupancy from $1d_{3/2}$ and $2s_{1/2}$ orbital for both $sdba$ and $psdmk$-interactions is smaller in comparison to that form $1d_{5/2}$ orbital. The distributions of ^{38,40,42} S have the configurations of $\left[(1s)^4(1p)^{12}\right]$ inert core. The occupancies of $1d_{5/2}, 1d_{3/2}, 2s_{1/2}, 1f_{7/2}, 1f_{5/2}, 2p_{3/2}$ and $2p_{1/2}$ proton and neutron orbital with sdpfk and sdpfuinteractions are shown Figs. (2, c) and (2, d). The contribution of neutron occupancy from $1d_{5/2}$ is dominant for both $sdpfk$ and $sdpfu$-interactions.

Table 1: The calculated excitation energies Ex with $sdba$ and $psdmk$ interactions for $^{32-36}$S-isotopes, and with $sdpfk$ and $sdpfu$ interactions for $^{38-42}$S-isotopes are compared with the measured values of Ref. [18].

$_{16}$S AN	$E_{x.cal}$ (MeV)		$E_{x.exp}$ (MeV)
	$Sdba$	$psdmk$	
32, 16	1.600	3.613	2.230(15)
34, 18	1.684	2.292	2.127(13)
36, 20	2.044	6.275	3.290(3)
	$Sdpfk$	$sdpfu$	
38,22	1.552	1.459	1.292(2)
40,24	0.855	0.942	0.903(7)
42,26	0.910	0.998	0.890(15)

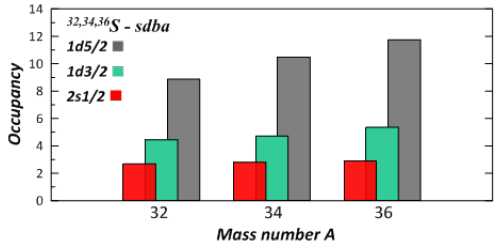

Figure (2-a): Bar chart of the Occupancies of 1 $d_{5/2}$, 2 $s_{1/2}$ and 1 $d_{3/2}$ valence proton and neutron orbital (^{16}O is the core) for ^{32,34,36} S with *sdba*-interaction.

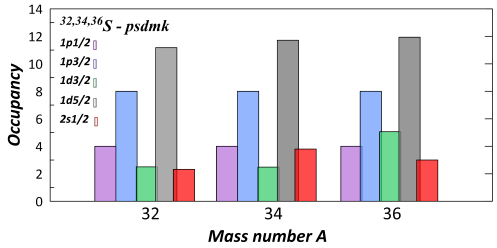

Figure (2-b): Bar chart of the Occupancies of $1p_{1/2}$, $1p_{3/2}$, 1 $d_{5/2}$, 2 $s_{1/2}$ and 1 $d_{3/2}$ valence proton and neutron orbital (^{4}He is the core) for ^{32,34,36} S with $p \leq dmk$-interaction.

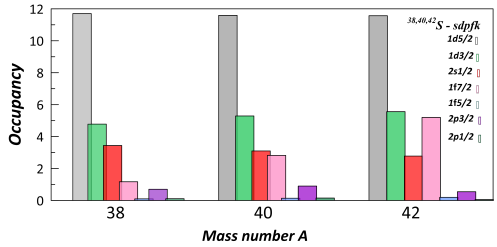

Figure (2-c): Bar chart of the Occupancies of 1 $d_{5/2}$, 1 $d_{3/2}$, 2 $s_{1/2}$, $1f_{7/2}$, $1f_{5/2}$, $2p_{3/2}$ and $2p_{1/2}$ valance proton and neutron orbital (^{16}O is the core) for ^{38,40,42}S with *sdpfk* interaction.

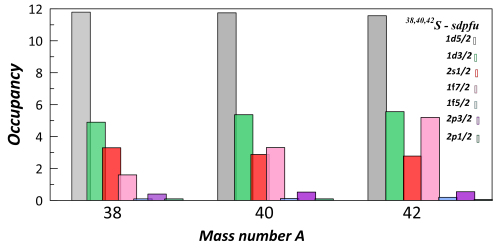

Figure (2-d): Bar chart of the Occupancies of 1 $d_{5/2}$, 1 $d_{3/2}$, 2 $s_{1/2}$, $1f_{7/2}$, $1f_{5/2}$, $2p_{3/2}$ and $2p_{1/2}$ valance proton and neutron orbital (^{16}O is the core) for ^{38,40,42} S with *sdpfu* interaction.

The calculations of the quadrupole moment for Sulfur-isotopes are presented in table (2) in comparison with the available experimental data of Ref. [27]. This comparison is shown in Fig. (3).The proton and neutron effective charges are varied to test their effects on the calculated quadrupole moments using different interactions. The results are performed with bare proton and neutron charges ($e_p = 1.0 \quad e$, $e_n = 0.0e$), the standard effective charges $\left(e_p^{eff} = 1.36e, e_n^{eff} = 0.45e\right)$ [22], and with $B-M$ effective proton and neutron charges [1]. There is reasonable agreement between the measured and calculated Q moments for the most isotopes using $(B-M)$ effective charges. The *psdmk*-interaction with $(B-M)$ effective charges gives good agreement with the experimental data for ^{32,34} S in both magnitude and sign. The results of *psdmk*-interaction for ^{32} S with (ST) and $(B-M)$ effective charges are $Q_{\text{cal}} = -12.79\ efm^2$ and -14.13efm^2 respectively. These values give a good agreement with the measured value $Q_{\text{exp}\equiv} = -16.2(2)efm^2$[30] and predicted oblate deformation as shown in Fig.(2). The results of *sdba*− interaction with (ST) and $(B-M)$ effective charges (14.38efm ^{2} and 15.89efm^2 respectively) reproduce the measured value in magnitude with opposite sign. The results for ^{34} S using *sdba* and *psdmk*− interaction with (ST) effective charges are $\left(1.18\text{efm}^2 \text{ and } 1.71\text{efm}^2\right)$, respectively, and underestimated the measured value $\left(+4.0 \pm 3\text{efm}^2\right)$, while those with $(B-M)$ effective charges are $\left(2.23\text{efm}^2 \text{ and } 2.19\text{efm } 2\right)$, respectively and give a reasonable agreement with measured values within the experimental error. These results refer to prolate deformation. The prolate deformation of ^{34} S nucleus is confirmed by both calculations except the obtained value with *sdba*-interaction for bare charge $\left(-0.22\text{efm}^2\right)$. The results for ^{36} S with all calculations refer to the slightly oblate deformation. In general, the extended psd-model space with ($B-M$) effective charges provides a reasonable agreement between the calculated and measured quadrupole moments for the majoring of this isotopes as shown in Fig. (3). The values of quadrupole moments for ^{38,40,42} S are presented in table (2). The calculations are performed for sdpfcross shell isotopes using *sdpfk* and *sdpfu*-interaction with proton $\left[(sp)^8(sd)^{z^{-12}}\right]$ and neutron $\left[(spsd)^{20}(pf)^{n-20}\right]$ configurations. The results of sdpfu-interaction with $(B-M)$ effective charges for ^{38} S$\left(-\ 8.13\text{efm}^2\right)$ and for ^{40} S $\left(-17.07\text{efm}^2\right)$ provide very good agreement with the results of Ref. [19] with clearly oblate deformation as shown in Fig. (3). The quadrupole moments for ^{42} S with both (ST) and (B-M) effective charges for *sdpfk*-interaction are (-6.8efm ^{2} and $-6.3efm^2$), respectively, and for *sdpfu*− interaction are (-18.7efm ^{2} and -17.8efm^2), respectively. These values are close to each other with small (large) oblate deformation for *sdpfk* (sdpfu)-interaction. Since no measured values of Q moment for this chain of $^{38-42}$ S-isotopes, the present results can be examined with the measured $B(E2)$ values which appear in well description as will be seen next. In general, an accurate and comprehensive description of the deformation of sulfur isotopes is attained with $(B-M)$ effective charges for sdpfu-interaction.

Table 2: Calculated quadrupole moments of the ^{32,34,36} S isotopes using *sdba*-interaction for the sd-model space, and *psdmk*-interaction for the *psd*-model space in comparison with the experimental values [30], and for ^{38,40,42} S isotopes using *sdpfk* and *sdpfu* interactions for the *sdpf*-model space in comparison with the available theoretical results [31].

$_{16}$S A, N	*b (fm)*	*Valence nucleons*		B-Meff. ch.		$Q_{calc.}$ $(e.fm^2)$						$Q_{exp.}(e.fm^2)$ [30]
		sd	*psd*	e_p^{eff}	e_n^{eff}	*sdba-Int.*			*psdmk-Int.*			
						Bare ch.	ST eff. ch.	B-M eff. ch.	Bare ch.	ST eff. ch.	B-M eff. ch.	
32, 16	1.884	16	28	1.180	0.820	7.946	14.38	15.89	-7.065	-12.79	-14.13	-16.0 (2.0)
34, 18	1.899	18	30	1.149	0.754	-0.22	1.18	2.23	0.46	1.71	2.19	+4.0 (3.0)
36, 20	1.913	20	32	1.122	0.695	-9.68	-13.17	-10.87	-6.57	-11.8	-7.38	-
						sdpfk-Int.			*sdpfu-Int.*			Q other Studies $(e.fm^2)$ [31]
		sdpf				*ST eff. ch.*	*B-M eff. ch.*		*ST eff. ch.*	*B-M eff. ch.*		
38, 22	1.927	22		1.098	0.643	-11.02	-11.89		-7.93	-8.13		-8.64
40, 24	1.941	24		1.076	0.596	-18.15	-18.69		-16.77	-17.07		-17.05
42, 26	1.953	26		1.056	0.553	-6.8	-6.3		-18.7	-17.8		-

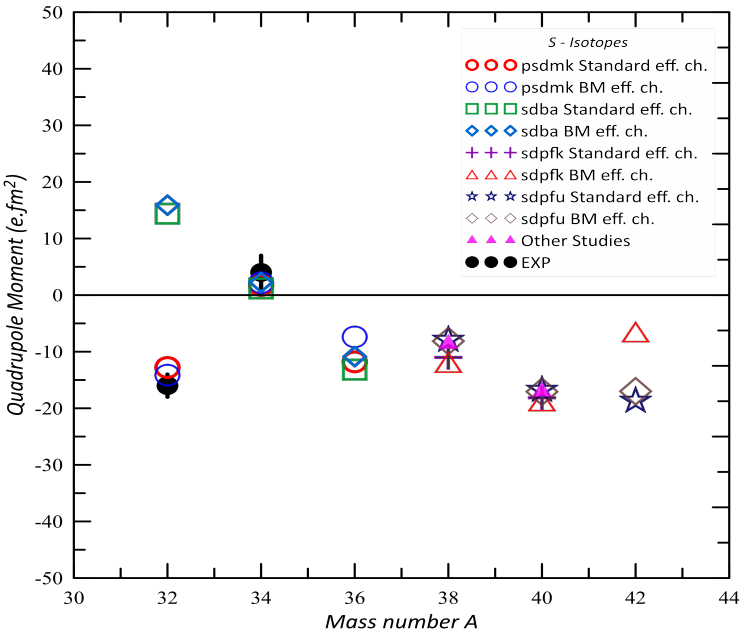

Figure 3: The theoretical and experimental electric quadrupole moments $Q(e.fm^2)$ for Sulfur-isotopes. The experimental data and other studies are taken from Ref. [27, 19].

Information concerning on the predicted $B(E2)$ strength and quadrupole deformation β_2 are indicated in table (3) compared with available experimental data. The measured $B(E2)$ strengths of Ref. [18, 21] and recently of Ref. [14] are used to test in detail the predictions of the present calculations using different interactions with $(B-M)$ effective charges. In Fig. (4), the *psdmk* and *sdba*-interactions fail to reproduce the measured $B(E2)$ strengths and deformation β_2 for $^{32-36}$ S. The results of *psdmk*-interaction are underestimated and roughly half of the measured values, while those of sdba-interaction are overestimated by about a factor of 2 , except for ^{36} S nucleus with closed shell of $N = 20$, the value of $B(E2)\left(114.9e^2fm^4\right)$ is close to the measured value $\left(104 \pm 28e^2fm^4\right)$ of Ref. [21]. The observed disagreement in $B(E2)$ values may be related to the proton and neutron model space utilized in this calculations. The results for $^{38-42}$ S (with $N > 20$) for both calculations nicely confirm the measured values of $B(E2)$ and β_2 of Ref. [18] within the experimental uncertainties. The results of $sdpfu-$ interaction have greatly improved the description of the measured $B(E2)$ of Ref. [18] within the experimental error. The comparison of the predicted $B(E2)$ and β_2 with those measured are shown in Fig. (4) and Fig. (5), respectively. Fig. (6), indicates the deformation parameter β_2 as a function of the $B(E2)$ strength for $^{32-42}$ S. The bar chart in this figure shows that the small value of deformation β_2 (0.126) obtained at least value of $B(E2)\left(56.96e^2fm^4\right)$ for ^{36} S isotope with $N = 20$ which reflects the nearly spherical shape for ^{36} S. The deformation β_2 clearly affected by $B(E2)$ strength values (see table 3). One can conclude that the nuclei with neutron number (N) far from magic number normally having deformed shape, while the nuclei with N-closed shell leads to spherical symmetry of charge distribution lie with spherical shape close the

stability region.

Table 3: The calculated reduced transition probabilities and the deformation parameters for psd cross-shell and *sd*-shell with *psdmk* and *sdba* interactions respectively for $^{32-36}$ S isotopes, also for *sdpf* cross-shell with *sdpfk* and *sdpfu* interactions for $^{38-42}$ S isotopes compared with the experimental data [14, 18, 21].

$_{16}SA, N$	$Ex_{cal.}(MeV)$		$B(E2)_{exp.}$ [28]	$B(E2)_{exp.}$ [12,32]	Exexp. (MeV) [28]	$B(E2)_{Cal.}$		$\beta_{2exp.}$ [28]	$\beta_{2cal.}$	
	sdba	*psdmk*				*psdmk*	*sdba*		*psdmk*	*sdba*
32,16	1.600	3.613	2.230(15)	300(13)[32]	295.8^{+85}_{-44}	156.6	667.2	0.3102^{+44}_{-23}	0.226	0.40
34,18	1.684	2.292	2.127(13)	212(12)[32]	208.3(120)	122.6	437.1	0.250(7)	0.192	0.362
36,20	2.044	6.275	3.290(3)	104(28)[32]	$88.6 + 87_{-52}$	56.96	114.9	0.1569^{+77}_{-46}	0.126	0.179
	sdpfk	*sdpfu*				*sdpfk*	*sdpfu*		*sdpfk*	sdpfu
38,22	1.522	1.459	1.292(2)	235(30)[32] 299(19)[12]	235(30)	270.8	236.6	0.247(16)	0.265	0.248
40,24	0.855	0.942	0.903(7)	334(36)[32] 284(26)[12]	334(36)	412.3	381.1	0.284(15)	0.316	0.304
42,26	0.910	.998	0.890(15)	400(6)[32] 326(48)[12]	397(63)	480.1	408.2	0.300(24)	0.330	0.308

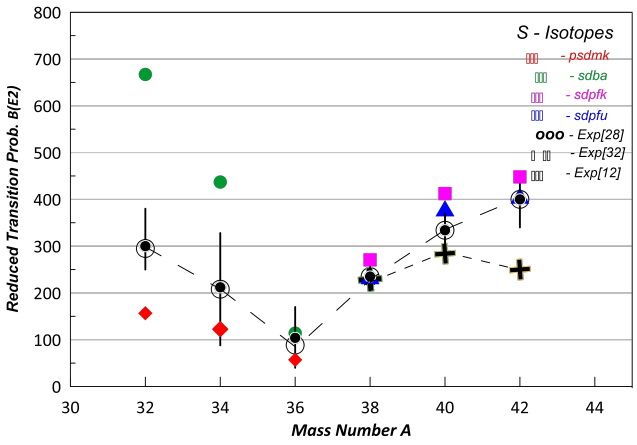

Figure 4: Reduced transition probabilities for even-even S-isotopes as a function of mass number A. The experimental data are taken from Ref. [18, 21, 14].

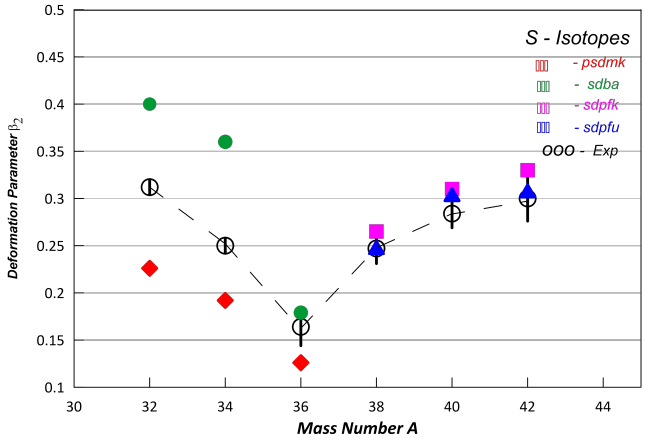

Figure 5: Deformationparameters β_2 for even-even S-isotopes as a function of mass number A. The experimental data are taken from Ref [18].

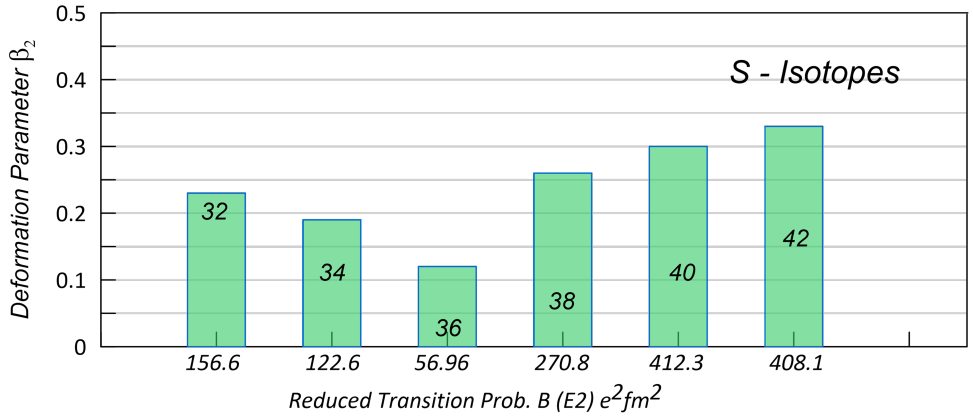

Figure 6: Bar chart of the deformation parameters with the reduced transition probabilities for $^{32-42}$S-isotopes

The comparison of the measured B($E2$) strengths of the Ref. [18] (black tableau) and the B($E2$) strengths predicted using different interactions for several 2^+states is indicated in Fig. (7). The results for ^{34} S using *psdmk*-interaction (red tableau) for excitation energy 2^+state at 2.292MeV is only in good agreement to the measured value 2.127 ± 13MeV of $Ref.$[28], and B($E2$) strength $122.6e^2fm^4$ is lower than the measured value $212 \pm 12e^2fm^4$ of Ref. [21] and $208.3 \pm 120e^2fm^4$ of Ref. [18], by about a factor of 1.7. While the B($E2$) strength using sdba-interaction (437.1 e^2fm^4 at 1.684MeV)(green tableau) is about of factor 2 higher than the measurement value. For ^{32} S, the *psdmk*-interaction predicted 156.6e^2fm^4 B($E2$) strength at 3.613MeV lower than the measured value $300 \pm 13e^2$fm^4 of Ref.[32] by about a factor of 1.9, while the predicted value 667.2e^2fm^4 at 1.6MeV of sdba-interaction is about a factor of 2.2 larger than the measured value. For ^{36} S, the B($E2$) strength with the *sdba* interaction $114.9e^2fm^4$ is reasonably improving the agreement with the measured value $104 \pm 28e^2fm^4$, while the B($E2$) strength value with the *psdmk*-interaction is reduced to be 56.96e^2fm^4 and roughly half of the measured value. This discrepancies in the excitation energies and B($E2$) strengths for $^{32-36}$ S with both interactions are visual in Fig.(7-a). Fig.(7-b) shows good agreement in both shape and magnitude of the excitation energies and B($E2$) strengths between the measured values of Ref.[28,32] and the present results especially with the results of *sdpfu*-interaction from S-isotopes with $N > 20$.

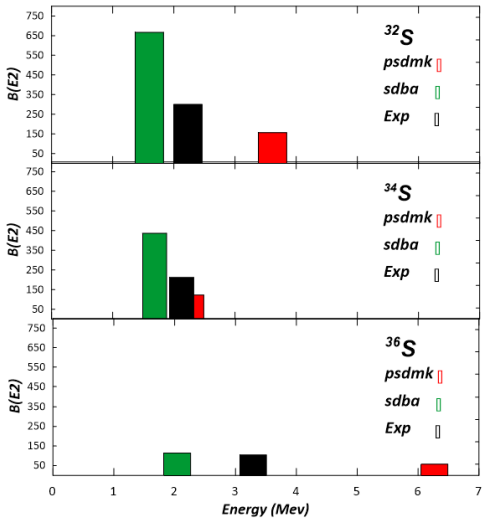

Figure (7-a): Reduced transition probabilities $B(E2; 0_1^+ \rightarrow 2_1^+)$ strengths in the $^{32-36}$S-isotopes as a function of Excitation energies compared with the experimental data of Ref [28].

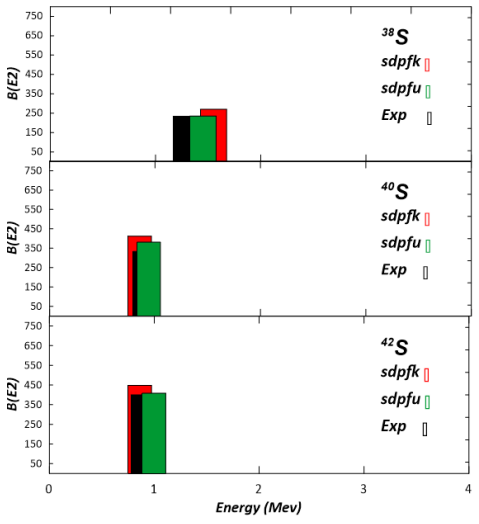

Figure (7-b): Reduced transition probabilities $B(E2; 0_1^+ \rightarrow 2_1^+)$ strengths in the $^{3-42}$S-isotopes as a function of Excitation energies compared with the experimental data of Ref. [18].

The inelastic longitudinal form factor can provide more detailed description for the electromagnetic properties of nuclei. The inelastic $C2$ form factors for 2_1^+excited state of S-isotopes using different interactions are presented in Fig. (8-a, b). The CP effects are included with $(B - M)$ effective charges. Each one represents three predictions curves

(solid and dash curves), the black curves for ^{32} S $\left(^{38}\text{ S}\right)$, red curves for ^{34} S $\left(^{40}\text{ S}\right)$ and green curves for ^{36} S $\left(^{42}\text{ S}\right)$. The influences of the nuclear deformation on the C2 form factor are also indicated. The results of the isotopes with $N \leq 20$ using *sdba*-interaction (solid curves) and using psdmk-interaction (dashed curves) are compared with the available experimental data [31] of ^{32} S and shown in Fig. (8-a). The results of cross-shell isotopes with $N > 20$ using the sdpfk-interaction (solid curves) and sdpfu-interaction (dashed curves) are shown in Fig. (8-b), where no experimental data are available. Inspection these curves reveals that the diffraction minima shift inward and outward for isotopes with more neutrons. The calculated C2 form factor using sdba-interaction for ^{32} S (black solid curve) overestimates the experimental data for all reigns of (q). The psdmk-interaction (black dashed curve) provides a reasonable agreement with the experimental data up to $q > 2.5fm^{-1}$, and reproduces very well the location of the first diffraction minimum. The C2 form factors of ^{32} S and ^{34} S with *sdba*-interaction are dominated at low q-region with first diffraction minimum located at $q = 1.65\text{fm}^{-1}$, and the second diffraction minimum is located at $q = 3.7\text{fm}^{-1}$for^{32} S and at $q = 4.14\text{fm}^{-1}$ for ^{34} S. This is due to the higher values of nuclear deformation ($\beta_2 = 0.4$ and $\beta_2 = 0.36$, respectively) compared with the lower values of *psdmk*-interaction ($\beta_2 = 0.226$ and 0.192, respectively). For ^{36} S-isotpes, the first diffraction minimum for *sdba*-interaction is located at q-region closely to that of ^{32,34} S isotopes and coincident for *psdmk*-interaction. The second diffraction minimum disappears for both *sdbq* and *psdmk* interactions, this is due to the lower values of ($\beta_2 = 0.17$ and 0.126), respectively. This relative decrease of β_2 is attributed to the nuclei be closer to the neutron magic number $N = 20$. The nuclear deformation β_2 has a significant influence on the changing trend of C2 form factor of ^{34,36} S isotopes chain with mass number A increasing, the second diffraction minima from sdba-interaction have outward shift at higher q-region, and the β_2 decreasing (see Fig. (8-a)). The C2 longitudinal form factors of $^{38-42}$ S-isotopes chain are presented in Fig. (8-b). No experimental data are available for C2 transition in this chain. The results of sdpfu-interaction (dashed curves) coincide with the results of sdpfk-interaction for ^{38} S and ^{40} S at $0.1 < q < 3.2\text{fm}^{-1}$. The first diffraction minimum is located of $q = 1.54$ fm^{-1} for both isotopes, while the second diffraction minimum is approximately disappeared. The C2 form factor of ^{42} S using sdpfk interaction (solid green curve) provides two diffraction minima. The first diffraction minimum is located at $q = 3.15\text{fm}^{-1}$, which is due to the nuclear deformation. With the values of β_2 increasing, as well as the mass numbers increasing, the second diffraction minimum of ^{42} S from sdpfk-interaction has inward shift which is the opposite from the results of Fig. (8-a).

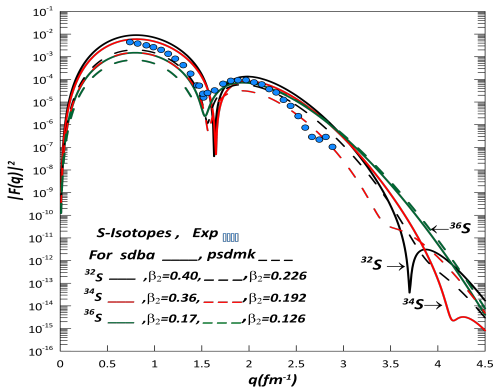

Figure (8-a): Inelastic longitudinal C2 form factors for ^{32,34,36}S-isotopes using psdmk and sdba interactions. The experimental data of ^{32}S are taken from Ref. [31].

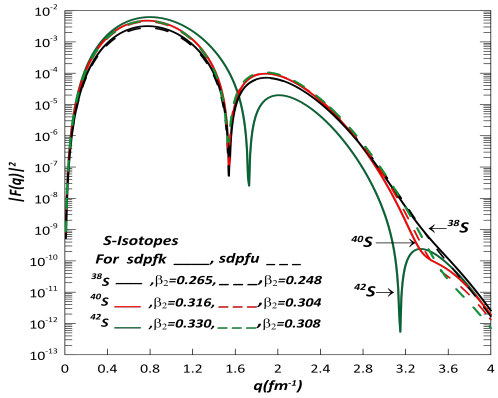

Figure (8-b): Inelastic longitudinal C2 form factors for ^{38,40,42}S-isotopes using sdpfk and sdpfu interactions.

4 Conclusions

Besides testing the scope of different model spaces with different interactions, the present analysis for the $^{32-42}$ S isotopes shows a strong contribution of $ld_{5/2}$ orbit. The contribution of neutron occupancy from $Id_{5/2}$ is dominant for all adopted interactions. The predictions of the Q moments provide a discriminating test and can lead to improve the wave functions and models. For all C2 transitions, the inclusion of effective charges are adequate to obtain a good agreement between the predicted and measured quadrupole moments. For Q moments of $^{32-36}$ S isotopic chain, $(B - M)$ effective charges with psdmk-interaction give well agreement with the measured values in both magnitude and sign. For $^{38-42}$ S isotopic chain, the present results with $sdpfu$-interaction give good predictions of Q moments and coincide with the other theoretical study, since there is no available data. The discrepancies in the excitation energies and B($E2$) strengths for $^{32-36}$ S with both interactions are clearly appeared, while good agreement especially with the $sdpfu$-interaction are shown for $^{38-42}$ S-isotopic chain. The present results investigate the changing trends

of C2 form factors from deformation parameters β_2, and reveals that the diffraction minima shift inward and outward for isotopes with more neutrons.

References

[1] A.N. Bohr and B.R. Mottelson, *Nuclear Structure (in 2 volumes)*, World Scientific Publishing Company, 1998.

[2] B.A. Brown, R. Radhi and B.H. Wildenthal, *Electric quadrupole and hexadecupole nuclear excitations from the perspectives of electron scattering and modern shell-model theory*, Phys. Rep. **101** (1983), no. 5, 313–358.

[3] B.A. Brown, A. Arima and J.B. McGrory, *E2 core-polarization charge for nuclei near 16O and 40Ca*, Nuclear Phys. A **277** (1977), no. 1, 77–108.

[4] B.A. Brown, A. Etchegoyen and N.S. Godwin, *WDM rae, WA Richter, WE Ormand, EK Warburton, JS Winfield, L. Zhao, and CH Zimmerman*, Tech. Rep. MSU-NSCL-1289, National SuperConducting Cyclotron Laboratory, 2004.

[5] P.J. Brussaard and P.W.M. Glaudemans, *Shell-model applications in nuclear spectroscopy*, North-Holland Publishing Company, 1977.

[6] T. Forest Jr and J. Dirk Walecka, *Electron scattering and nuclear structure*, Adv. Phys. **15** (1966), no. 57, 1–109.

[7] T.W. Donnelly and J.D. Walecka, *Electron Scattering and Nuclear Structure*, Ann. Rev. Nuclear Sci. **25** (1975), no. 1, 329–405.

[8] T.W. Donnelly and I. Sick, *Elastic magnetic electron scattering from nuclei*, Reviews of modern physics **56** (1984), no. 3, 461.

[9] J.P. Elliott and T.H.R. Skyrme, *Centre-of-mass effects in the nuclear shell-model*, Proc. Royal Soc. London. Series A. Math. Phys. Sci. **232** (1955), no. 1191, 561–566.

[10] T. Glasmacher, B.A. Brown, M.J. Chromik, P.D. Cottle, M. Fauerbach, R.W. Ibbotson, K.W. Kemper, D.J. Morrissey, H. Scheit and D.W. Sklenicka, *Collectivity in 44S*, Phys. Lett. B **395** (1997), no. 3-4, 163–168.

[11] J.P. Glickman, W. Bertozzi, T.N. Buti, S. Dixit, F.W. Hersman, C.E. Hyde-Wright, M.V. Hynes, R.W. Lourie, B.E. Norum and J.J. Kelly, *Electron scattering from Be 9*, Phys. Rev. C **43** (1991), no. 4, 1740.

[12] .K Kaneko, Y. Sun, T. Mizusaki and M. Hasegawa, *Shell-model study for neutron-rich sd-shell nuclei*, Phys. Rev. C **83** (2011), no. 1, 014320.

[13] E. Kwan, C.Y. Wu, N.C. Summers, G. Hackman, T.E. Drake, C. Andreoiu, R. Ashley, G.C. Ball, P.C. Bender and A.J. Boston, *Precision measurements of the B (E1) strengths in 11Be*, Fission and Properties of Neutron-Rich Nuclei, World Scientific, 2014, pp. 678–681.

[14] B. Longfellow, D. Weisshaar, A. Gade, B.A. Brown, D. Bazin, K.W. Brown, B. Elman, J. Pereira, D. Rhodes and M. Spieker, *Quadrupole collectivity in the neutron-rich sulfur isotopes S 38, 40, 42, 44*, Phys. Rev. C **103** (2021), no. 5, 054309.

[15] D.J. Millener and D. Kurath, *The particle-hole interaction and the beta decay of 14B*, Nuclear Phys. A **255** (1975), no. 2, 315–338.

[16] F. Nowacki and A. Poves, *New effective interaction for $\theta h\omega$ shell-model calculations in the sd-pf valence space*, Phys. Rev. C **79** (2009), no. 1, 014310.

[17] T. Otsuka, A. Gade, O. Sorlin, T. Suzuki and Y. Utsuno, *Evolution of shell structure in exotic nuclei*, Rev. Mod. Phys.**92** (2020), no. 1, 015002.

[18] B. Pritychenko, M. Birch, B. Singh and M. Horoi, *Tables of E2 transition probabilities from the first 2+ states in even–even nuclei*, At. Data Nucl. Data Tables **107** (2016), 1–139.

[19] R.A. Radhi, A.A. Alzubadi and A.H. Ali, *Magnetic dipole moments, electric quadrupole moments, and electron scattering form factors of neutron-rich s d-p f cross-shell nuclei*, Phys. Rev. C **97** (2018), no. 6, 064312.

[20] R.A. Radhi, Z.A. Dakhil and N.S. Manie, *Microscopic calculations of quadrupole moments in Li and B isotopes*, Eur. Phys. J. A **50** (2014), no. 7, 1–9.

[21] S. Raman and C.W. Nestor, *Jr., and P. Tikkanen*, At. Data Nucl. Data Tables **78** (2001), no. 1, 43.

[22] W.A. Richter, S. Mkhize, and B Alex Brown, *sd-shell observables for the USDA and USDB Hamiltonians*, Phys. Rev. C **78** (2008), no. 6, 064302.

[23] H. Sagawa and B.A. Brown, *E2 core polarization for sd-shell single-particle states calculated with a skyrme-type interaction*, Nuclear Phys. A **430** (1984), no. 1, 84–98.

[24] A. Saxena, A. Kumar, V. Kumar, P.C. Srivastava and T. Suzuki, *Ab initio description of collectivity for sd shell nuclei*, Hyperfine Interact.**240** (2019), no. 1, 1–8.

[25] H. Scheit, T. Glasmacher, B.A. Brown, J.A. Brown, P.D. Cottle, P.G. Hansen, R. Harkewicz, M. Hellström, R.W. Ibbotson and J.K. Jewell, *New region of deformation: The neutron-rich sulfur isotopes*, Phys. Rev. Lett. **77** (1996), no. 19, 3967.

[26] O. Sorlin and M.-G. Porquet, *Nuclear magic numbers: New features far from stability*, Prog. Part. Nuclear Phys. **61** (2008), no. 2, 602–673.

[27] N.J. Stone, *Table of nuclear magnetic dipole and electric quadrupole moments*, At. Data Nuc. Data Tables **90** (2005), no. , 75–176.

[28] L. Jo Tassie and F.C. Barker, *Application to electron scattering of center-of-mass effects in the nuclear shell model*, Phys. Rev. **111** (1958), no. 3, 940.

[29] Y. Utsuno, T. Otsuka, B.A. Brown, M. Honma, T. Mizusaki and N. Shimizu, *Shape transitions in exotic Si and S isotopes and tensor-force-driven Jahn-Teller effect*, Phys. Rev. C **86** (2012), no. 5, 051301.

[30] T.R. Werner, J.A. Sheikh, M. Misu, W. Nazarewicz, J. Rikovska, K. Heeger, A.S. Umar and M.R. Strayer, *Ground-state properties of exotic Si, S, Ar and Ca isotopes*, Nuclear Phys. A **597** (1996), no. 3, 327–340.

[31] B.H. Wildenthal, B.A. Brown and I. Sick, *Electric hexadecupole transition strength in S 32 and shell-model predictions for E4 systematics in the sd shell*, Phys. Rev. C **32** (1985), no. 6, 2185.

[32] S.-G. Zhou, *Structure of exotic nuclei: a theoretical review*, arXiv preprint arXiv:1703.09045 (2017).